CCFE
CULHAM CENTRE FOR FUSION ENERGY

UK Atomic Energy Authority

UKAEA-CCFE-PR(18)43

K.G. McClements

Reconnection and fast particle production in tokamak and solar plasmas

Reconnection and fast particle production in tokamak and solar plasmas

K.G. McClements[1]

[1]CCFE, Culham Science Centre, Abingdon, Oxfordshire OX14 3DB, UK

This is a preprint of a paper submitted for publication in
Advances in Space Research

Reconnection and fast particle production in tokamak and solar plasmas

K.G. McClements[1]

CCFE, Culham Science Centre, Abingdon, Oxfordshire OX14 3DB, UK

Abstract

Detailed *in situ* studies of magnetic reconnection and particle acceleration, which play a crucial role in the release and redistribution of energy in solar flares, can be performed in tokamak plasmas under conditions resembling those of the flaring solar corona. Recent measurements and modelling of fast particle production during reconnection events in the Mega-Amp Spherical Tokamak (MAST) are described. Specifically, observations in this device of electron acceleration during edge localised modes, and of both ion and electron acceleration during merging-compression plasma start-up, are presented, and possible implications of these studies for particle acceleration in flares are discussed. The results from MAST lend weight to the conjecture that large numbers of ions are accelerated to sub-MeV energies in flares.

1. Introduction

Laboratory devices designed specifically for the study of basic plasma physics processes, such as the Large Plasma Device (LaPD) at UCLA (Gekelman et al. 2016), have provided valuable insights into the physics of magnetic reconnection. However, it is challenging to replicate the plasma conditions in the flaring solar corona, for example in terms of collisionality and plasma beta. Tokamak plasmas (whose ultimate purpose is electricity production via thermonuclear fusion) are typically characterised by higher energy densities than dedicated reconnection experiments, and have dimensionless parameters, such as plasma beta, that are similar to those of the corona (see e.g. Table 1 in Fundamenski et al. 2007). Such devices therefore provide an opportunity to study processes likely to be operating in flares, with a spatial resolution (sub-ion Larmor radius) that will probably never be achievable in solar physics, and with very high time resolution (down to less than 1 μs).

After an overview of tokamak plasmas aimed at non-fusion specialists in Section 2, the present paper describes recent studies of reconnection and particle acceleration associated with two specific phenomena, edge localised modes (ELMs: section 3) and merging-compression plasma start-up (section 4), in the Mega-Amp Spherical Tokamak (MAST) at the Culham Science Centre in the UK. Possible implications of these studies for particle acceleration in flares are discussed in section 5, followed by concluding

[1]ken.mcclements@ukaea.uk, +44 1235 466303

remarks in section 6.

2. Overview of tokamak plasmas

Tokamaks (Wesson 2004) are axisymmetric toroidal plasmas in which the toroidal component of the magnetic field B_φ is usually dominant, and is generated mainly by currents in external coils. The poloidal componant of the field B_θ, on the other hand, is generated primarily by the toroidal plasma current I_p. Consequently the evolution of B_θ (unlike that of B_φ) is determined largely by plasma physics rather than engineering parameters.

In common with the solar corona, tokamak plasmas are characterised by electrical resistivity η that is low in the sense that the Lundquist number $S = 4\pi c_A L/\eta c^2$ (c_A and c being respectively the Alfvén speed and speed of light) is invariably much larger than unity if the length scale L is identified with the macroscopic system size (Priest 1982, Fundamenski et al. 2007). In both coronal and tokamak plasmas, these macroscopic lengths are also much larger than kinetic scales (electron and ion Larmor radii and skin depths). For these reasons, ideal magnetohydrodynamics (MHD) generally holds to a good approximation, but can cease to be applicable as a result of instabilities generating gradients with length scales approaching resistive or kinetic values, leading to magnetic reconnection. The presence of a large toroidal field in tokamaks also helps to ensure that, as in the flaring corona, the plasma beta $\beta = 8\pi nkT/B^2$ is generally smaller than unity, although the values of the plasma parameters in β are somewhat different from those in the corona: plasmas in MAST typically had temperature T, particle density n and total magnetic field B of the order of, respectively, 10 MK, $3 \times 10^{13}\,\mathrm{cm}^{-3}$ and 4 kG (Turnyanskiy et al. 2009). The absolute global length scales in flares are, of course, enormous compared to those in tokamaks (thousands of km compared to a few metres at most), but it is likely that particle acceleration is determined primarily by the kinetic scales mentioned above, and for these parameters the ratios of solar coronal values to tokamak values are much closer to unity (Fundamenski et al. 2007).

Another obvious difference between tokamak and flare plasmas is that in the former the magnetic field lines in almost the entire plasma form a set of closed, nested, toroidal surfaces (Fig. 1), whereas in the latter the coronal magnetic field is connected to the much denser and cooler chromosphere and photosphere. One should always bear in mind this fundamental difference in global magnetic topology when comparing the two situations. The reason for having closed magnetic surfaces in tokamaks is, of course, that they are needed to ensure adequate confinement of charged particles, as illustrated by the ion orbit in Fig. 1. However, there is always an outermost surface of closed magnetic flux (indicated by the blue curve in Fig. 1), beyond which there is a "scrape-off layer" (SOL) of plasma exhausted from the closed flux region. In most currently-operating tokamaks, the magnetic field lines in the exhaust plasma are connected to a "divertor", a solid surface at the top or bottom of the vacuum vessel. The SOL magnetic field topology thus resembles to some extent that of a flaring coronal loop, with the divertor playing the role of the photosphere.

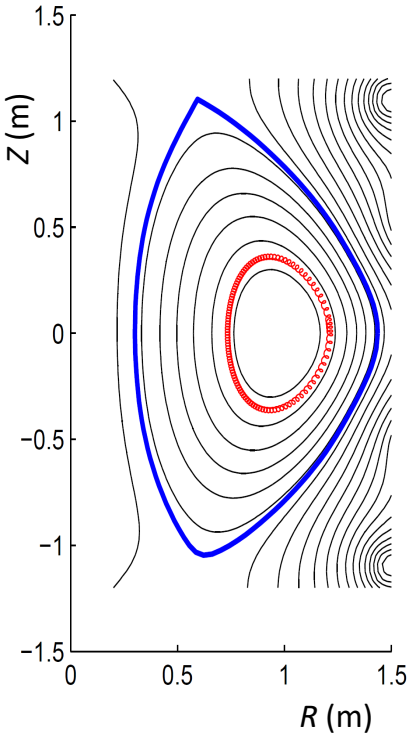

Figure 1: Poloidal cross-section of a MAST plasma, showing magnetic flux surfaces (black curves), the last closed flux surface (blue curve) and a typical ion orbit (red curve). Major radius R is distance from the torus axis of symmetry, while Z represents vertical distance from the vacuum vessel midplane.

3. Particle acceleration during edge localised modes

There is a regime of relatively high plasma confinement in tokamaks, referred to as *H-mode* and characterised by a "pedestal" region of steep pressure gradient near the plasma edge. An ELM is a periodic instability driven by this pressure gradient, and identified as a short-lived ($< 100\,\mu$s) spike in deuterium Balmer-alpha (Dα) emission caused by the expulsion of plasma filaments, with density and temperature that are characteristic of the H-mode pedestal (deuterium was the main ion species in the majority of MAST plasmas). Links have previously been drawn at the fluid level between ELMs and flares, with both being attributed to a nonlinear, explosive ideal MHD instability (Cowley et al. 2003, Fundamenski et al. 2007). These links, combined with the demonstrable importance of fast particles in the energetics of flares (see e.g. Emslie et al. 2004, Krucker et al. 2010), provide an obvious motivation to search for evidence of magnetic reconnection and particle acceleration during ELMs.

Such evidence has indeed emerged from tokamak experiments, most clearly in the form of bursts of radiation at microwave frequencies. The magnetic fields and particle densities used in tokamaks are such that the electron cyclotron frequency $\Omega_e/2\pi$ and electron plasma frequency $\omega_{pe}/2\pi$ generally lie in this range. As in radio astronomy,

the intensity of microwave emission from tokamak plasmas is often quantified using the temperature T_b of an optically-thick black body producing the same radiation intensity at that frequency. During ELMs in MAST T_b values of between 3 and 4 orders of magnitude above the pre-ELM thermal value were detected (Freethy et al. 2015). For reference, the temperature at the top of the pedestal in H-mode MAST pulses was typically about 1 MK, and the electron temperature across the plasma (determined by firing a laser into the plasma and detecting the resulting Thomson-scattered light) was never more than about a factor of ten or so higher than this. It is very likely therefore that brightness temperatures of the order measured during ELMs resulted from a collective instability driven by strongly supra-thermal electrons. As illustrated in Fig. 2, the bursts typically peaked in intensity a few tens of microseconds before the Dα emission, suggesting that electrons were being accelerated to supra-thermal energies during the early stages of ELM filament eruption. Correlations between ELMs and microwave bursts have been observed in some other tokamaks, including TFTR (Taylor et al. 1992) and, more recently, DIII-D (Li et al. 2017).

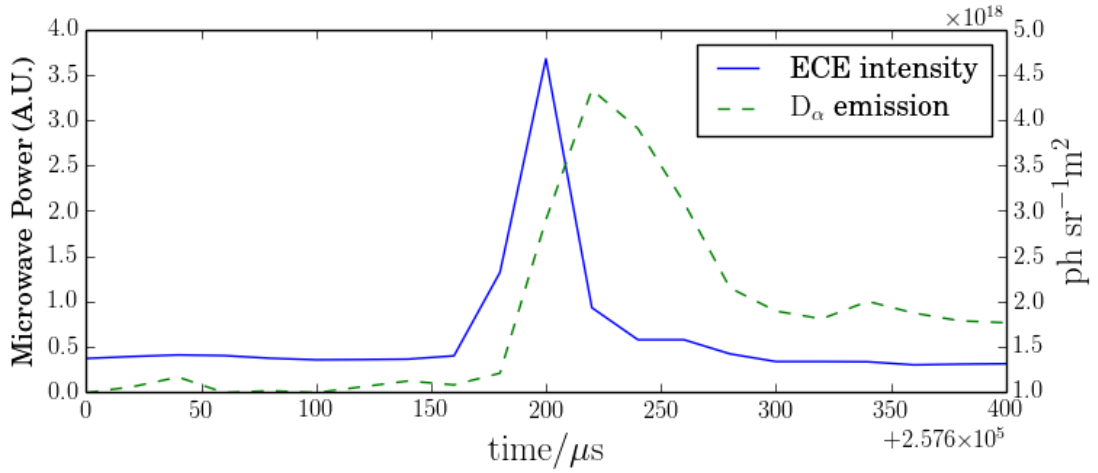

Figure 2: Evolution of microwave intensity (solid curve) and deuterium Balmer-alpha emission (dashed curve) during a typical ELM in MAST (reproduced with permission from Freethy et al. 2015).

ELMs in MAST were also often accompanied by bursts of soft X-ray emission (photon energies in the approximate range 1-30 keV) from the plasma edge: an example is shown in Fig. 3. It can be seen that the X-ray peak again occurs a few tens of microseconds before that of the Balmer-alpha emission. Thus, the microwave and X-ray bursts were essentially simultaneous. The latter can be attributed to nonthermal bremsstrahlung due to a small fraction of the local electron population having energies in excess of the soft X-ray diagnostic threshold (Freethy et al. 2015).

Strong correlations between microwave and hard X-ray bursts are also routinely observed in solar flares (Tan and Tan 2012). Moreover delays between flare X-ray bursts and Balmer-alpha emission, similar to that shown in Fig. 3, have been recorded (Radziszewski et al. 2011). The delays fall into two groups, with longer delays (up to

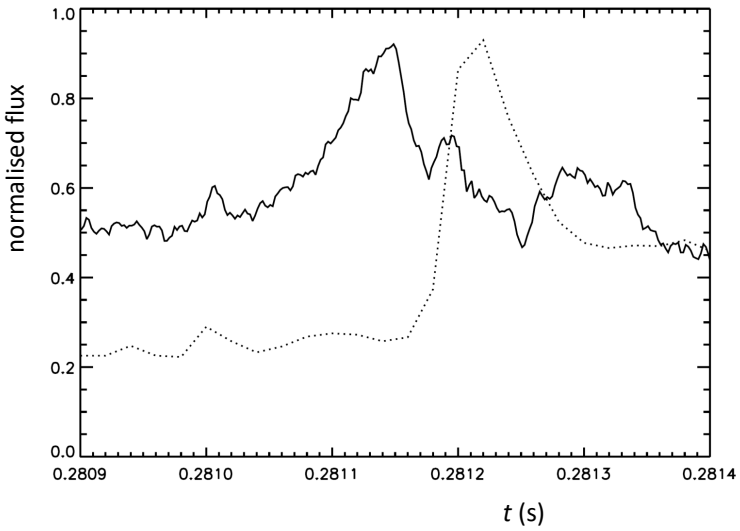

Figure 3: Evolution of normalised soft X-ray intensity (solid curve) and deuterium Balmer-alpha intensity (dotted curve) during a typical ELM in MAST. The X-ray intensity corresponds to a line-of-sight passing through the low field side plasma edge above the midplane.

about 18 s) being attributed to the propagation of thermal conduction fronts at the local ion sound speed to the chromosphere, where neutrals are present in sufficient numbers to account for the Balmer-alpha emission. The timescales appear to be consistent with the usual picture of primary flare energy release and electron acceleration occurring in a coronal loop-top source, the released energy then taking a finite time to reach the denser, cooler parts of the solar atmosphere.

Due to the global nature of the instability driving ELMs, simulations of this phenomenon generally employ fluid rather than kinetic models. The best tool currently available for this is the nonlinear resistive MHD JOREK code (Pamela et al. 2013). Simulations of ELM filaments in MAST using this code have revealed the presence of edge-localised parallel electric fields of up to 0.07 statvolt cm^{-1}, persisting for long enough to accelerate electrons to energies in the tens of keV range, thereby creating the conditions required for X-ray bursts to occur via electron-ion bremsstrahlung (Freethy et al. 2015). In the first instance, acceleration due to parallel electric fields is likely to result in strongly field-aligned energetic electron distributions. The subsequent evolution of such distributions in a plasma with bulk parameters corresponding to the pedestal region in MAST has been simulated using a particle-in-cell code, EPOCH (Lai et al. 2015). When the energetic electron tail extends to velocities that are sufficiently large compared to the bulk electron thermal speed, the growth rate of the anomalous Doppler instability (ADI) exceeds the Landau damping rate, resulting in the generation of waves at frequencies close to those of the observed microwave bursts (Freethy et al. 2015). The ADI causes pitch angle scattering of field-aligned energetic electrons on timescales of a few hundred electron cyclotron periods (corresponding to tens of

nanoseconds), resulting in a much more isotropic (but still energetic) distribution. The fact that the microwave and soft X-ray emission both decay on timescales of a few tens of μs (compare Figs. 2 and 2) suggests that the energetic electrons have a similar (i.e. very short) confinement time in the plasma. It is evident that the acceleration site is already close to the region of confined magnetic flux, and so energetic electrons do not have to be transported very far across flux surfaces to enter the SOL, at which point they are rapidly lost from the plasma: the propagation time of a 10 keV electron along the magnetic from the MAST midplane to the divertor is less than a microsecond.

The time delays between different radiation signatures in ELMs and flares, noted above, suggest that in both cases energetic electrons propagate along open field lines prior to the peaks in Balmer-alpha emission. In tokamaks there is generally a steep rise in neutral density beyond the last closed-flux surface, and it is believed that most of the energy transfer in ELMs occurs via plasma filaments rather than energetic particles. It is likely that the delays between fast electron radiation signatures and Balmer-alpha emission in Figs. 2 and 3 are due to the radial propagation of filaments rather than energetic electron timescales. In this respect, the longer class of delays in flares identified by Radziszewski et al. (2011) perhaps provide a closer analogue to those observed in ELMs, in that both can be attributed to bulk plasma processes. The absolute timescales in flares are, of course, much longer than those in ELMs, due to a difference of about six orders of magnitude in the magnetic field connection lengths.

4. Particle acceleration during plasma startup

Detailed descriptions of merging-compression plasma start-up in MAST have been provided by Stanier et al. (2013) and Tanabe et al. (2015). In summary, plasma rings with parallel toroidal currents were formed around coils located above and below the vessel midplane, subsequently detaching and merging in the midplane of the vacuum vessel (corresponding to $Z = 0$ in Fig. 1) due to their mutual attraction. A change of magnetic field line topology (i.e. reconnection) from two tori to a single torus with nested magnetic surfaces typically occurred around 4-5 ms after the start of the pulse. Observations of ion acceleration during this process were obtained in early MAST campaigns using a neutral particle analyser (NPA), which detected atoms resulting from charge-exchange between high energy ions and neutrals. The MAST NPA had a single horizontal line-of-sight, which could be changed from pulse to pulse. The line-of-sight was in the vacuum vessel midplane, and was specified by the major radius R_{NPA} of its closest approach to the toroidal symmetry axis (cf. Fig. 1). Although, as noted previously, deuterium was usually the dominant ion species in MAST plasmas, some hydrogen was always present, and it was possible to measure separately neutral fluxes of the two species. The NPA has 39 energy channels for both species, ranging up to several tens of keV, making it possible to measure the fast ion distribution function.

The NPA was most commonly used to study the behaviour of fast ions resulting from the injection into the plasma of high-energy neutral beams. However, beam injection was generally not applied until after the merging start-up phase, and therefore no fast ions of external origin were present in the plasma at this time. At the start of the merg-

ing phase (around 4 ms into the pulse), bursts of high energy protons and deuterons were detected, lasting for a few milliseconds. The highest fluxes were recorded when R_{NPA} was comparable to the major radius ($\simeq 0.7$ m) at which the plasma rings are believed to have merged, suggesting that the fast ions originated from this location and were strongly aligned with the magnetic field. Fig. 4 shows fast ion spectra obtained by integrating the NPA fluxes over a period of 6 ms, covering the whole of the merging phase. In calculating these spectra, the energy-dependence of the charge-exchange cross-section was taken into account, and therefore they provide a true measure of the *in situ* fast ion distributions, rather than the distributions of neutrals. Note that a log-linear scale is used, so that a Maxwellian energy distribution would appear as a straight line. It can be seen that the typical energy gain of protons is higher than that of deuterons, as expected for acceleration resulting from a transient parallel electron field. The slope given by the two lowest energy points in the deuterium spectrum (the red curve) correspond to a temperature of about 2 MK, which is a realistic bulk ion temperature in the later stages of the merging process (Tanabe et al. 2015). Identifying these points with the bulk deuterium distribution, it is possible to establish that the fraction of deuterons accelerated was rather low in this case, of the order of 10^{-4} (McClements et al. 2018).

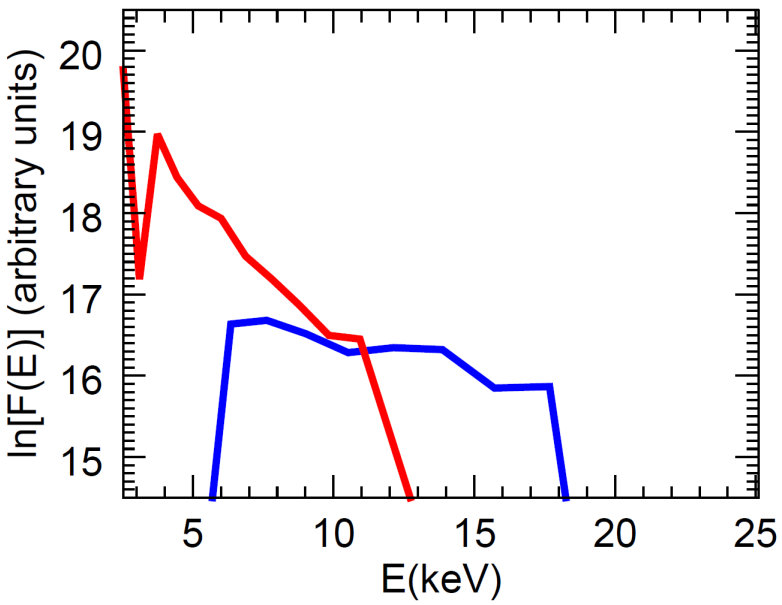

Figure 4: Deuterium (red) and hydrogen (blue) energy spectra recorded by the MAST NPA during the merging phase of pulse 9153 (reproduced with permission from McClements et al. 2018).

In later MAST campaigns, microwave bursts were detected in many pulses at the same time ($t \sim 4 - 5$ ms) as fast ions in the early campaigns (McClements et al. 2018). The emission was short-lived (less than 150 μs) and narrow-band ($\Delta\nu/\nu \leq 0.1$), peaking at frequencies ν of the order of the electron cyclotron frequency. The burst intensities were up to 3 orders of magnitude in excess of background levels, strongly implying the presence of supra-thermal electrons. As in the case of the ELM bursts,

EPOCH simulations suggest that the bursts could have been driven by field-aligned fast electrons via the ADI (McClements et al. 2018), although no clear evidence has been found for such electrons during the early merging phase in either soft X-ray or Thomson scattering data.

It was not possible to measure directly electric fields resulting from merging compression in MAST, but quantitative information on the fields likely to have been generated can be gleaned from fluid simulations of this process reported by Stanier et al. (2013). The model employed by these authors included a generalised Ohm's law with Hall, electron pressure, resistive and hyper-resistive terms. The maximum parallel electric field at the merging point was significantly higher in Hall-MHD simulations than in pure MHD simulations, but in the former case it was found to be insensitive to the assumed hyper-resistivity, reaching values of around 0.3 statvolts cm^{-1} and remaining at a high level for about a microsecond. Another striking feature of the Hall-MHD simulations (not observed in the MHD simulations) was the formation of magnetic islands in the vicinity of the merging point. This phenomenon has often been observed in non-MHD simulations of reconnection, including some that were specifically intended to model the flaring solar corona (see e.g. Threlfall et al. 2012). Since the merging point is likely to be the site of particle acceleration, it is probable that the presence of magnetic islands affects the acceleration process. Direct measurements during merging reconnection in MAST (Tanabe et al. 2015) show that electron heating occurred initially in a very localised region, whose extent is comparable to or smaller than the ion skin depth $\delta_i = c/\omega_{pi} \sim 20\,\mathrm{cm}$ (c being the speed of light and ω_{pi} the ion plasma frequency). It is clear therefore that MHD is not sufficient to describe the reconnection process. This may also be true of flares, although it is impossible to be certain, since it is not possible to resolve length scales as small as δ_i in the corona.

The simulations reported by Stanier et al. (2013) prompted McClements et al. (2018) to suggest a simple model for the reconnecting fields, in which the poloidal magnetic flux ψ (defined such that the poloidal magnetic field is $\nabla\psi \times \nabla\varphi$, where φ is toroidal angle in right-handed (R, φ, Z) coordinates) in the vicinity of the merging point is given by

$$\psi = \psi_0 e^{-t^2/\tau^2} \exp\left\{-\frac{(R-R_0)^2}{\delta R^2} - \frac{Z^2}{\delta Z^2}\right\}, \tag{1}$$

where the constants ψ_0, τ, δR and δZ determine the magnitude, duration and spatial localisation of the field perturbations associated with the reconnection process. The black curves in Fig. 1 show contours of a time-independent (or very slowly-varying) ψ that defines the magnetic equilibrium state after the merging-compression process has been completed. The assumed time-dependence of the ψ given by Eq. (1) produces an inductive toroidal electric field, whose magnitude can be chosen to match the values occurring in the fluid simulations. McClements et al. (2018) tracked test particle protons and deuterons in fields corresponding to this poloidal flux, using parameters that were consistent with experimental measurements and the simulations, and obtaining fast ion distribution functions that were in close agreement with those shown in Fig. 4 in terms of the maximum energies of each species. If particle motions (including drifts) perpendicular to the magnetic field are neglected, together with the mirror force arising from longitudinal variations in the field, it is straightforward to integrate the parallel

component of the ion equation of motion to obtain the final energy of an ion of mass m_i and charge e initially at rest at $R = R_0$, $Z = 0$:

$$\mathcal{E} = \frac{e^2\psi_0^2}{2m_i R_0^2}. \tag{2}$$

Using a value of ψ_0 that is consistent with the poloidal flux that is known to be destroyed in the merging process, we obtain from Eq. (2) maximum energies of 24.8 keV for protons and 12.4 keV for deuterons, broadly in line with the particle spectra shown in Fig. 4. We thus have an explanation for the highest particle energies recorded by the NPA during the merging process, and for the result that protons are accelerated to higher energies than deuterons.

The simple calculation used above does not explain the absence of evidence for supra-thermal electrons in soft X-ray or Thomson scattering data: the argument that reconnection during merging causes light particles to be accelerated to higher energies than heavy ones should apply *a fortiori*, one might suppose, to electrons. The lack of evidence for very high energy electrons may be at least partly because of instrumental threshold effects. If only a small fraction of the electron population were accelerated, as in the case of the ions, we would not expect such electrons to be revealed by Thomson scattering measurements, since the scattering process would be dominated by bulk electrons, and a small number of energetic electrons would produce only noise in the data. The intensity of any soft X-ray bremsstrahlung resulting from the slowing-down of energetic electrons by bulk ions would also be low if the accelerated electron fraction were small. Moreover the bulk plasma density during the early merging phase of MAST plasmas was typically an order of magnitude lower than in the main phase of the pulse: since the bremsstrahlung flux is proportional to both the fast particle density and the bulk density, the X-ray flux would thus be relatively low during merging. Enhancements in soft X-ray emission have in fact been detected during the latter stages of the merging process, but these can be attributed to bulk electron heating and a rise in plasma density, since the electron temperature and density inferred from Thomson scattering data also rose during this period.

In the fluid modelling reported by Stanier et al. (2013) and the kinetic modelling reported by McClements et al. (2018) the merging plasma was assumed to be toroidally symmetric. If, as seems likely, the magnetic field was actually three-dimensional and disordered, this could have limited the acceleration process, since field fluctuations give rise to cross-field diffusion of particles out of the acceleration region, at a rate that is proportional to their parallel velocity, the magnetic field scale length L_B, and the square of the field fluctuation level, $\delta B/B$ (Rechester and Rosenbluth 1978). This diffusivity can be used to infer the critical fluctuation level above which particles of energy $\mathcal{E}$ stop accelerating (McClements et al. 2018):

$$\left(\frac{\delta B}{B}\right)_{\rm crit} = \left(\frac{\delta Z^2 e E_\parallel}{2\mathcal{E}L_B}\right)^{1/2}, \tag{3}$$

where δZ has been assumed to be smaller than δR. Since mass does not appear in Eq. (3), the maximum particle energy for a given fluctuation level is the same for electrons

and ions. Thus, magnetic field stochasticity provides a possible explanation for the fact that runaway acceleration of the entire electron population was not observed during merging, while the non-observation of energetic electrons via soft X-ray emission may be due to the bremsstrahlung flux being below the instrumental threshold, as suggested above. The microwave bursts detected during merging provide strong evidence that some electrons were nevertheless accelerated to strongly supra-thermal energies.

5. Implications for solar flares

Energetic ions most commonly arise in tokamak plasmas through a combination of external agents, such as neutral beam injection (NBI) or injection of waves in the ion cyclotron range of frequencies (ICRF), and fusion reactions. NBI, ICRF waves or a combination of these are routinely used to achieve high plasma performance, making it difficult to study the acceleration of ions from the bulk distribution, for example during the ELMs discussed in section 3 (these instabilities occur only in H-mode, which could not be achieved in MAST without the use of NBI). The best opportunities for such studies are thus presented by "Ohmic" plasmas, without external sources of fast ions (the temperatures that are achievable in such plasmas are also relatively low, which means that thermonuclear sources of fast ions are usually negligible). The MAST NPA recorded bursts of energetic deuterons and protons not only during the Ohmic merging phase, as described in the previous section, but also during internal reconnection events in the main phase of some entirely Ohmic pulses (Helander et al. 2002). Generally, high energy ions can be detected with relative ease in tokamak plasmas. In addition to the NPA method described above, such ions can be detected via direct losses from the plasma, neutron emission, Doppler-shifted Balmer-alpha emission, or through instabilities that are known to be driven by fast ions, such as toroidal Alfvén eigenmodes (see e.g. McClements and Fredrickson 2017). Energetic electrons in tokamaks are usually detected via their X-ray, γ-ray or microwave radiation signatures, although their presence is also sometimes revealed through the excitation of instabilities (Valovič et al. 2000).

In contrast, accelerated ions in flares can only be detected easily at energies in excess of about 1 MeV, via γ-ray or neutron emission (Emslie et al. 2004). Energetic ions of solar origin can also be observed directly in the interplanetary medium, but these provide only limited information on flare acceleration processes since their properties may have been strong affected by fields in the interplanetary medium. Test particle simulations of ion acceleration in flares generally produce monotonic-decreasing particle spectra that extend down to thermal energies (see e.g. Fig. 4 in Dalla and Browning 2008), suggesting that it is difficult to find a mechanism capable of accounting for flare γ-ray and neutron observations that does not also produce large numbers of sub-Mev fast ions. Such ions, being predominantly protons in a predominantly hydrogen bulk plasma, do not produce measurable fluxes of neutrons, unlike most of the fast ion species in tokamak plasmas. The evidence for energetic electrons in flares, of which there is plenty, mainly takes the form of X-ray, γ-ray and radio/microwave data, as in tokamaks, and indeed the emission mechanisms are believed to be very similar. Decimetric spike

bursts during flares, for example, are normally attributed to a collective instability driven by non-Maxwellian energetic electron distributions (Melrose and Wheatland 2016), as in the case of the microwave bursts observed in MAST during ELMs and merging-compression start-up.

To see how fast ion energies measured during merging in MAST could scale to flares, we note that the momentum gained by an ion of mass m_i in time Δt due to an inductive parallel electric field $E_\parallel$ is $m_i \Delta v_\parallel = eE_\parallel \Delta t$, and Faraday's law gives a simple relation between $E_\parallel$ and the poloidal magnetic field ΔB that must be annihilated to produce it, together with the perpendicular scale length of the electric field, $L_\perp$:

$$E_\parallel \simeq (L_\perp/c)\Delta B/\Delta t. \tag{4}$$

Parameter values that are applicable to merging-compression in MAST are $\Delta B = 1\,\mathrm{kG}$ and $L_\perp = 20\,\mathrm{cm}$. As discussed earlier, the latter is of the order of the ion skin depth in the pre-merging plasma, and it is also comparable to the measured length scale of strong electron heating (Tanabe et al. 2015). Eq. (4) then yields an energy gain of 10 keV for protons and 5 keV for deuterons, similar to the measured values (see Fig. 4). Similar or higher ion energy gains would occur in flares if, say, a 10 G magnetic field were to be annihilated in a reconnecting region with a perpendicular length scale in excess of $2 \times 10^3\,\mathrm{cm}$. This value of $L_\perp$ is comparable to the ion skin depth in coronal active regions, and the measurements and modelling of merging-compression in MAST suggest that this may be the relevant length scale to use for describing flare reconnection. The same parameters applied to electrons would imply particle energies that were higher than the figures quoted here by a factor of m_i/m_e where m_e is the electron mass, but, as in MAST, it is possible that the particle energies resulting from reconnection in flares are limited by cross-field particle transport resulting from magnetic field stochasticity. Indeed it has been proposed that such a process determines the perpendicular length scales of solar coronal loops (Galloway et al. 2007).

6. Concluding remarks

Particle acceleration has been observed during edge localised modes (ELMs) and merging plasma start-up in the MAST tokamak, under plasma conditions similar to those of the flaring solar corona. ELMs in MAST and flares have several features in common, including the acceleration of electrons to energies in the tens of keV range, resulting in bursts of microwave and X-ray emission, and delays between the first appearance of fast electrons and bursts of Balmer-alpha emission from plasma regions distant from the site of particle acceleration. Fast particle measurements during merging plasma start-up in MAST suggest that parallel electric fields arising from magnetic reconnection can be at least as effective in producing fast ions as fast electrons. Given the similarities between plasma conditions during merging in MAST and those in the flaring corona, it seems likely that large numbers of sub-MeV ions are being accelerated, undetected, in flares. The generally-accepted interpretation of flare hard X-ray emission already requires a large fraction of the total energy released to reside in energetic electrons (see e.g. Krucker et al. 2010): the theoretical problem of channelling magnetic field energy

into supra-thermal particles would of course be aggrevated if it were to be established conclusively that a substantial fraction of these particles were sub-MeV energetic ions.

Acknowledgments

This work has received funding from the RCUK Energy Programme [grant number EP/P012450/1]. To obtain further information on the data and models underlying this paper please contact PublicationsManager@ccfe.ac.uk.

References

Cowley, S.C., Wilson, H.R., Hurricane, O., Fong, B., 2003. Explosive instabilities: from solar flares to edge localized modes in tokamaks. Plasma Phys. Control. Fusion 45, A31-A38.

Dalla, S., Browning P.K, 2008. Particle trajectories and acceleration during 3D fan reconnection. Astron. Astrophys. 491, 289-295.

Emslie, A.G., Miller, J.A., Brown, J.C., 2004. An explanation for the different locations of electron and ion acceleration in solar flares. Astrophys. J. 602, L69-L72.

Freethy, S.J., McClements, K.G., Chapman, S.C., Dendy, R.O., Lai, W.N., Pamela, S.J.P., Shevchenko, V.F., Vann, R.G.L., 2015. Election kinetics inferred from observations of microwave bursts during edge localized modes in the Mega-Amp Spherical Tokamak. Phys. Rev. Lett. 114, 125004 (5pp).

Fundamenski, W., Naulin, V., Neukirch, T., Garcia, O.E., Juul Rasmussen, J., 2007. On the relationship between ELM filaments and solar flares. Plasma Phys. Control. Fusion 49, R43-R86.

Galloway, R.K., Helander, P., MacKinnon, A.L., 2007. Cross-field diffusion of electrons in tangled magnetic fields and implications for coronal fine structure. Astrophys. J. 646, 615624.

Gekelman, W., DeHaas, T., Van Compernolle, B., Daughton, W., Pribyl, P., Vincena, S., Hong, D., 2016. Experimental study of the dynamics of a thin current sheet. Phys. Scr. 91, 054002 (21pp).

Helander, P., Eriksson. L.-G., Akers, R.J., Byrom, C., Gimblett, C.G., Tournianski, M.R., 2002. Ion acceleration during reconnection in MAST. Phys. Rev. Lett. 89, 235002 (4pp).

Krucker, S., Hudson, H.S., Glesener, L., White, S.M., Masuda, S., Wuelser, J.-P., Lin, R.P., 2010. Measurements of the coronal acceleration region of a solar flare. Astrophys. J. 714 1108-1119.

Lai W.N., Chapman, S.C., Dendy, R.O., 2015. Velocity space evolution of a minority energetic electron population undergoing the anomalous Doppler instability. Phys. Plasmas 22, 112119 (7pp).

Li, E., Austin, M.E., White, R.B., Taylor, G., 2017. The build-up of energetic electrons triggering electron cyclotron emission bursts due to a magnetohydrodynamic mode at the edge of tokamaks. Phys. Plasmas 24, 092509 (6pp).

McClements, K.G., Fredrickson, E.D., 2017. Energetic particles in spherical tokamak plasmas. Plasma Phys. Control. Fusion 59, 053001 (22pp).

McClements, K.G., Allen, J.O., Chapman, S.C., Dendy, R.O., Irvine, S.W.A., Marshall, O., Robb, D., Turnyanskiy, M., Vann, R.G.L., 2018. Particle acceleration during merging-compression plasma start-up in the Mega-Amp Spherical Tokamak. Plasma Phys. Control. Fusion 60, 025013 (11pp).

Melrose, D.B., Wheatland, M.S., 2016. Is cyclotron maser emission in solar flares driven by a horseshoe distribution? Sol. Phys. 291, 36373658.

Pamela, S.J.P., Huijsmans, G.T.A., Kirk, A., Chapman, I.T., Harrison, J.R., Scannell, R., Thornton, A.J., Becoulet, M., Orain, F. the MAST Team, 2013. Resistive MHD simulation of edge-localized-modes for double-null discharges in the MAST device. Plasma Phys. Control. Fusion 55, 095001 (13pp).

Priest, E.R., 1982. Solar magnetohydrodynamics. Dordrecht: Reidel.

Radziszewski, K., Rudawy, P., Phillips, K.J.H., 2011. High time resolution observations of solar Hα flares - II Search for signatures of electron beam heating. Astron. Astrophys. 535, A123 (8pp).

Rechester, A.B., Rosenbluth, M.N., 1978. Electron heat transport in a tokamak with destroyed magnetic surfaces. Phys. Rev. Lett. 40, 38-41.

Stanier A., Browning P., Gordovskyy, M., McClements, K.G., Gryaznevich, M.P., Lukin, V.S., 2013. Two-fluid simulations of driven reconnection in the mega-ampere spherical tokamak. Phys. Plasmas 20, 122302 (12pp).

Tan, B., Tan, C., 2012. Microwave quasi-periodic pulsation with millisecond bursts in a solar flare on 2011 August 9. Astrophys. J. 749, 28 (8pp).

Tanabe, H., Yamada, T., Watanabe, T. Gi, K., Kadowaki, K., Inomoto, M., Imazawa, R., Gryaznevich, M., Michael, C., Crowley, B., Conway, N.J., Scannell, R., Harrison, J., Fitzgerald, I., Meakins, A., Hawkes, N., McClements, K.G., OGorman, T., Cheng, C.Z., Ono, Y., The MAST Team, 2015. Electron and ion heating characteristics during magnetic reconnection in the MAST spherical tokamak. Phys. Rev. Lett. 115, 215004 (5pp).

Taylor, G., Bush, C.E., Fredrickson, E.D., Park, H.K., Ramsey, A.T., 1992. Intense electron cyclotron emission bursts during high power neutral beam heating on TFTR. Nucl. Fusion 32, 1867-1872.

Threlfall, J., ParnelL, C.E., De Moortel, I., McClements, K.G., Arber, T.D., 2012. Nonlinear wave propagation and reconnection at magnetic X-points in the Hall MHD regime. Astron. Astrophys. 544, A24 (11pp).

Turnyanskiy M.R., Keeling, D.L., Akers, R.J., Cunningham, G., Conway, N.J., Meyer, H., Michael, C.A., Pinches, S.D., 2009. Study of the fast ion confinement and current profile control on MAST. Nucl. Fusion 49, 065002 (9pp).

Valovič, M., Lloyd, B., McClements, K.G., Warrick, C.D., Fielding, S.J., Morris, A.W., Pinfold, T., Wilson, H.R., COMPASS-D Team, ECRH Team, 2000. Quasi-stationary high β plasmas and fast particle instabilities in the COMPASS-D tokamak with ECRH and LHCD. Nucl. Fusion 40, 1569-1573.

Wesson, J., 2004. Tokamaks. Oxford: Oxford University Press (3rd edition).